

## Experimental Study of Laser-Induced Melting in Two-Dimensional Colloids

Q.-H. Wei, C. Bechinger, D. Rudhardt, and P. Leiderer

*Fakultät für Physik, Universität Konstanz, D-78434 Konstanz, Germany*

(Received 22 May 1998)

We study the phase behavior of a charged two-dimensional colloidal system in the presence of a periodic light field composed of two interfering laser beams. Above a certain light intensity, the light field initiates a liquid-solid transition. This effect is known as light-induced freezing. When the light field is increased above a critical value, however, the induced crystal is predicted to melt into a modulated liquid again. In this paper we report the first direct experimental observation of this reentrance phenomenon. [S0031-9007(98)07130-0]

PACS numbers: 82.70.Dd, 64.70.Dv

Freezing and melting are common but intriguing phenomena not only from the fundamental physical point of view but also from daily life experience [1]. The order distinguishing a liquid from a crystal is the spatial modulation of the particle density, which is homogeneous in the liquid phase while periodic in the crystalline solid phase. There still exist, however, some short-range structure or fluctuating density modes in liquids as indicated by the maximum in the structure factor at a nonzero wave vector. The freezing transition, which can be viewed as a condensation of the liquid density modes, is achieved, e.g., by lowering the temperature or increasing the particle density  $\rho$  of the system [1–3].

Chowdhury, Ackerson, and Clark demonstrated that if an external periodical potential is coupled to some of these density modes this may lead to a freezing transition of a liquid [4]. They subjected a two-dimensional (2D) system of strongly interacting colloidal particles to a one-dimensional (1D) potential provided by the standing wave pattern of two interfering laser beams. When the periodicity of the light pattern was chosen to be commensurate to the mean particle distance, the colloidal liquid was observed to crystallize if the light intensity is strong enough. This phenomenon is denoted as laser-induced freezing (LIF). A theoretical analysis in terms of the Landau-Alexander-McTague theory revealed that LIF may change from a first to a second order transition when the light intensity is increased [4].

When Chakrabarti *et al.* reinvestigated this phenomenon in terms of density functional theory and Monte Carlo simulations [5,6], they could reproduce the results of Chowdhury *et al.*, but additionally found a novel reentrant laser-induced melting transition (LIM) from the crystal to a modulated liquid phase when the light intensity is increased even further. It was suggested that this may be due to the restricted particle motion transverse to the potential modulation which would lead to a reduced effective dimensionality of the system and enhanced fluctuations.

In this Letter, we study the phase behavior of a two-dimensional system of strongly interacting colloidal particles under the influence of a modulated laser field

as a function of the light intensity. An analysis of the pair correlation function  $g(x, y)$  and the single particle density  $\rho(x, y)$  reveals that with increasing light intensity the system changes from a modulated liquid to a crystal, and finally back to a modulated liquid again. This is in agreement with the LIM phenomenon predicted above.

The samples used in our experiments consist of aqueous suspensions of polystyrene spheres 3  $\mu\text{m}$  in diameter and a polydispersity of 4% (Interfacial Dynamics Corp.). The particles are highly charged due to sulfate groups, leading to a strong repulsive screened Coulomb particle interaction. The sample cell was composed of two optical flats with a spacing of about 20  $\mu\text{m}$ . This narrow spacing is important to suppress thermal convection which is observed for spacings above a few hundred microns due to heating effects [7]. To control the particle interaction, the cell was connected to a circuit consisting of a peristaltically driven pump, a vessel containing ion exchange resin particles, and an electrical conductivity probe [8]. Additionally, a certain amount of ion exchange resin particles was added to the edge of the cell to stabilize our system during the experiments at an ionic conductivity of about 0.5  $\mu\text{S}/\text{cm}$ . We used a setup similar to the Mach-Zender interferometer to produce two parallel coherent laser beams from an Argon ion laser (TM00 mode,  $\lambda = 514 \text{ nm}$ ). These beams were directed by a convergent lens to cross and to produce interfering fringes in the plane of the sample which is located at the focal plane of the lens. A schematic picture of our system is shown in Fig. 1. The fringe spacing was adjusted by the spacing between these parallel beams through the position of a motor-driven mirror. The particles were additionally illuminated with white light from above and were observed with a CCD camera which was attached to an optical microscope. The scattered laser radiation was blocked with an optical high pass filter. The images were stored on videotape for further analysis. For details regarding our setup we refer to the literature [9].

To characterize the different structures we determined the pair correlation function  $g(x, y)$  and the single particle density  $\rho(x, y)$  from the coordinates of the particle centers

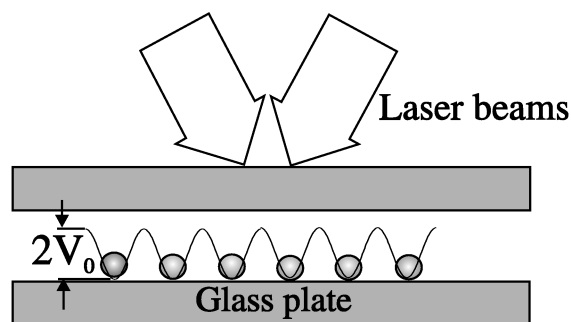


FIG. 1. Schematic representation of our sample geometry.

which were obtained by a particle recognition program. In particular,  $\rho(x, y)$  is an important and fundamental quantity directly displaying the spatial modulations and plays the role of an order parameter [1]. Thus, by qualitatively different functions for  $\rho(x, y)$ , one can distinguish different thermodynamic phases.

Since dielectric polystyrene particles are polarized by the electrical field of a laser beam, the interaction of these dipole moments with an interference pattern leads to a periodic, external potential for these particles. Taking the finite size of the colloidal spheres into account, the potential comprised by a modulated laser field can be written as [7]

$$V(x) = -V_0 \cos(2\pi x/d), \quad (1)$$

where  $V_0 = [3n_w P \sigma_0^3 (n^2 - 1) / c r_0^2 (n^2 + 2)] [j_1(\pi \sigma_0 / d) d / 2\pi \sigma_0]$ , with  $P$  being the laser power,  $c$  the velocity of light in vacuum,  $n$  the ratio of the refraction indices of polystyrene  $n_p$  and water  $n_w$ ,  $\sigma_0$  the colloidal particle diameter,  $j_1$  the first order spherical Bessel function,  $r_0$  the waist radius of the Gaussian laser beam, and  $d$  the period of the potential corresponding to the fringe spacing, respectively. In our setup,  $r_0$  was determined to  $350 \mu\text{m}$ . Since the averaged light intensity radially decreased from the center towards the edges due to the Gaussian shape of the laser beam, we considered only a central region of the interference fringes for our data analysis, which is about  $120 \mu\text{m}$  in diameter. The potential depth  $V_0$  in this region varied only about 5%; therefore Eq. (1) can be applied to good approximation. Dipole-dipole interactions between the particles can be neglected since they are only on the order of 1% of  $V_0$ .

The laser beams which were directed from above into our cell exerted additionally a vertical pressure on the particles, thus pushing them towards the bottom glass plate of the cell. However, since the glass surfaces are negatively charged when in contact with water, the particles are prevented from sticking to the glass surface by electrostatic repulsion [10,11]. The vertical radiation pressure reduced the fluctuations of the particles perpendicular to the cell plane which were estimated to be less than  $0.5 \mu\text{m}$  from the particle-wall potential [10,11] and makes our system two dimensional.

The particle density in our cell was kept constant with an area fraction of about 0.2, which is somewhat smaller than the concentration required for spontaneous crystallization. In the absence of a periodic light potential, the system therefore always exhibited a liquid structure, as can be seen from the homogeneous  $\rho(x, y)$  and isotropic  $g(x, y)$  in Figs. 2a and 2b. In contrast to this, considerable changes in the structure were observed, when a light potential was applied, as will be discussed in the following. Figs. 2c–2h show contour plots of  $\rho(x, y)$  and  $g(x, y)$  data for three different light intensities, corresponding to potentials  $V_0$  of  $0.6k_B T$ ,  $2.1k_B T$ , and  $6.3k_B T$ , respectively, where  $k_B T$  is the thermal energy at room temperature. To obtain sufficient statistics,  $\rho(x, y)$  and  $g(x, y)$  were averaged over 200 pictures having time intervals of 3 sec each. All length scales in Fig. 2 are in units of the potential period  $d$  which was kept constant at a value of  $8.3 \mu\text{m}$ . This periodicity is nearly commensurate with a hexagonal crystal structure with a lattice constant equal to the mean particle distance in the liquid phase, i.e., when  $V_0 = 0$ .

In Fig. 2c ( $0.6k_B T$ ), the particle density is modulated perpendicular to the interference fringes (oriented along the  $y$  direction) and reflect the underlying intensity pattern. In contrast, no modulations, i.e., a liquidlike behavior, are observed in the  $y$  direction. From the corresponding plot for  $g(x, y)$  it can be seen that correlation effects along the lines are only short ranged, and that a local hexagonal structure appears oriented according to the light potential. These features are characteristic for the modulated liquid phase.

Increasing the potential to  $2.1k_B T$ , one observes that now  $\rho(x, y)$  and  $g(x, y)$  are modulated both in the  $x$  and  $y$  directions, which shows that at this intensity the system responds by forming a 2D crystal (Figs. 2e and 2f). This is also in quantitative agreement with the LIF transition observed by other authors [4,7].

If the light intensity is increased even further to  $V_0 = 6.3k_B T$ , however, indications for crystalline order can no longer be found (Figs. 2g and 2h). Rather,  $\rho(x, y)$  and  $g(x, y)$  are again very similar to the modulated liquid phase observed in Figs. 2c and 2d. Obviously, enhancing the potential modulation causes the system to melt into a modulated liquid. This finding is in excellent agreement with the theoretically predicted light-induced melting. Furthermore, it can also be seen that the fluctuations in the  $y$  direction in this reentrant phase are much larger compared to the crystalline phase, which is also in agreement with theory [12]. A more detailed analysis shows that the width of the lines in Figs. 2c, 2e, and 2g, which reflects the transverse fluctuations of the particles, decreases with increasing light intensity. This is a direct consequence of an increased lateral confinement of the particles in the light potential wells.

More evidence for the assignment of the different phases mentioned above is derived from an analysis of

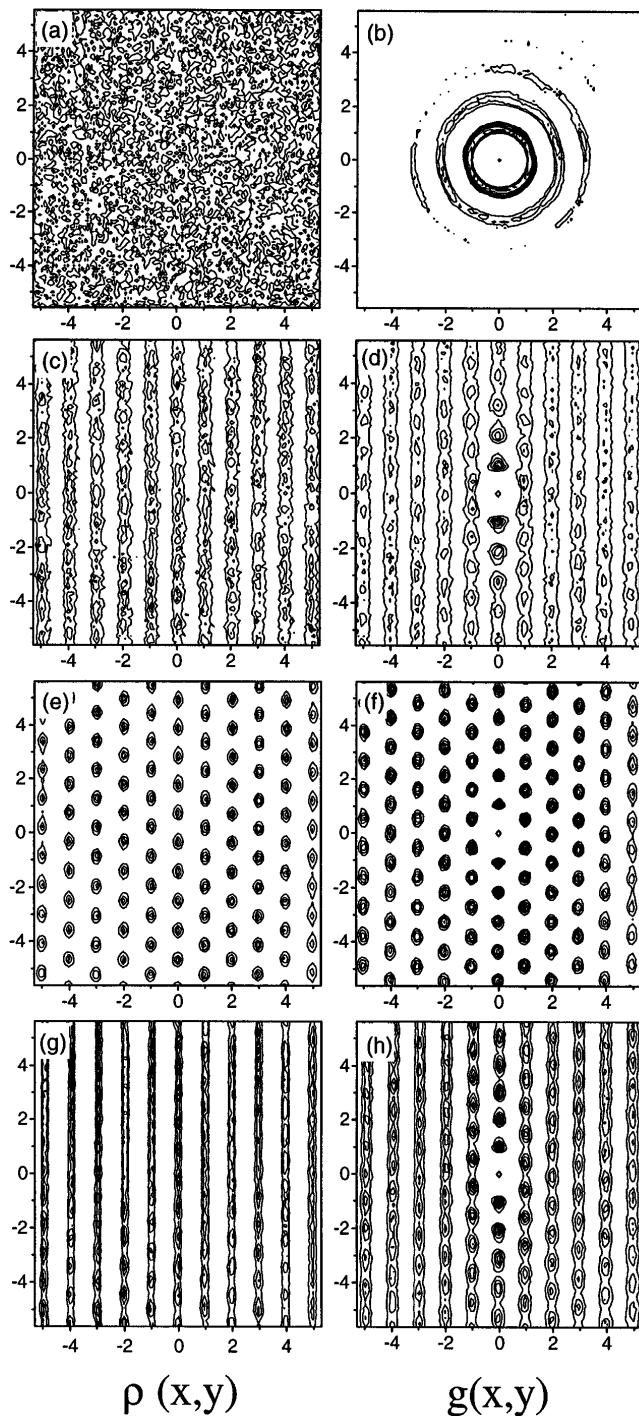


FIG. 2. Contour plots of the averaged density distribution  $\rho(x,y)$  and pair correlation function  $g(x,y)$  for zero light potential [(a),(b)] and for three nonzero potential values [{"(c),(d)  $0.6k_B T$  modulated liquid, [(e),(f)  $2.1k_B T$  crystal, and [(g),(h)  $6.3k_B T$  reentrant modulated liquid}]. The horizontal and vertical axes are  $x$  and  $y$ , respectively. All length scales are normalized by the potential period  $d$ .

the pair correlation function along the  $y$  direction  $g(y)$  as shown in Fig. 3. For the modulated liquid at the smallest light intensities, the particle correlation is short ranged

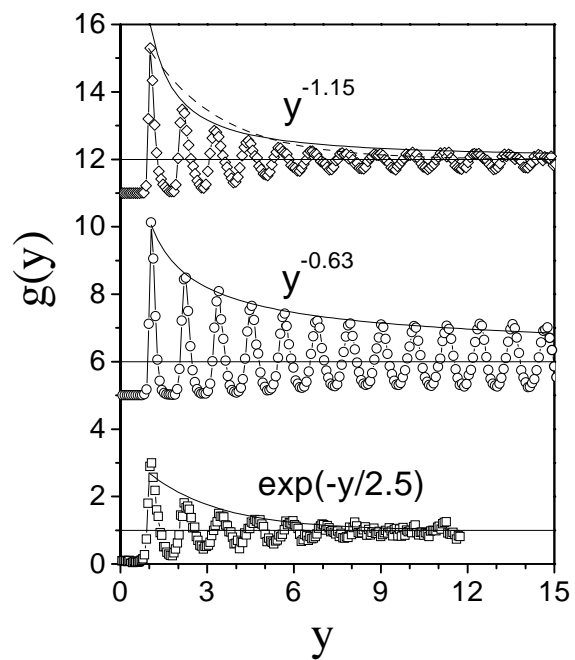


FIG. 3. Averaged pair correlation function  $g(y)$  of particles along the potential lines for  $V_0 = 0.6k_B T$  (squares),  $2.1k_B T$  (circles), and  $6.3k_B T$  (diamonds), respectively. The lines are fits as explained in the text. The data are offset in the vertical direction for clarity.

and finally decays to 1 with increasing  $y$  (squares). The envelope of this curve can be fitted to an exponential decay with a decay length of  $2.5d$  (solid line). This clearly demonstrates the liquid order of the particles in the  $y$  direction. At the intermediate potential, the pair correlation function decays much slower (circles) and its envelope cannot be described by an exponential decay. In contrast, we find that the data can be fitted well to an algebraic decay  $g(y) - 1 \sim y^{-\eta}$  with an exponent  $\eta = 0.63 \pm 0.05$  (solid line). This is in agreement with the fact that a 2D solid displays only quasi-long-range order and that the pair correlation function decays algebraically [13,14]. For a 2D solid with triangular lattice the exponent  $\eta$  at the melting point depends on the reciprocal lattice vector  $G$ . With  $G_0$  being the first reciprocal lattice vector,  $\eta$  is between  $1/4$  and  $1/3$  for  $G = G_0$ , and between  $3/4$  and  $1$  for  $G = \sqrt{3} G_0$ . The periodicity in our  $g(y)$  plot corresponds to  $G = \sqrt{3} G_0$ . The fact that we obtained a value for  $\eta$  smaller than the corresponding lower limit  $3/4$  indicates that the system was not at the melting point. For the highest potential used in our experiments ( $V_0 = 6.3k_B T$ ),  $g(y)$  decays much faster than in the crystalline state (diamonds). It is difficult to decide whether an algebraic (solid line) or an exponential function (dashed line) fits better to the data. However, unlike in the crystalline phase, the obtained algebraic exponent is now  $1.15 \pm 0.05$ , which is larger than the theoretical upper limit 1, indicating liquid order in the  $y$  direction.

The experimental determination of the LIM transition point is not easy because of the finite size of the system and the (theoretically predicted) continuous nature of the phase transition. Our data (including another data point, not shown here) suggest the LIM transition takes place between  $2.1k_B T$  and  $4k_B T$ , which is a factor of 5 to 10 times higher than the results of Monte Carlo simulations [6]. The same calculations, however, also predict the LIF transition to occur at much smaller values than observed both in our experiments and that of other authors [2,7]. This quantitative difference between theory and experiment might be partially attributable to the fact that the experiments were performed in finite size systems, whereas the simulation results are gained by extrapolation to the thermodynamic limit.

To understand the LIM from a microscopic point of view, it is helpful to first recall the mechanism of LIF: The short-range structure of 2D liquids is known to exhibit dominantly hexagonal order with random orientation [2]. An external 1D potential aligns this orientation and reduces the particle fluctuations perpendicular to the potential lines, thus leading to a long-range density mode in this direction (cf. Fig. 2d). When the light potential is strong enough, the interparticle repulsion results in a registration of particles in neighboring lines and, accordingly, in the formation of a crystal, i.e., in a LIF transition. It is important to pay attention to the fact that even in the crystalline state the particles fluctuate around their equilibrium positions (cf. Fig. 2e) which contributes also to the registration of particles and stabilizes the crystal. If now the fluctuations of particles perpendicular to the external potential lines are reduced by increasing the light intensity, the correlation between adjacent lines is partially lost, and the crystal melts to a modulated liquid. This LIM transition is not restricted to crystals formed by LIF but should be also observed in systems where the particle concentration is slightly above that for spontaneous crystallization [6].

The LIM phase transition observed here is a quite general phenomenon [15] and has already been shown in the theory of Nelson *et al.* for the phase transition of an adsorbate under the influence of a strong substrate potential [16]. It was predicted that the melting temperature of a so-called floating solid should decrease upon increasing the potential strength. This effect was not given attention before due to the fact that the strength of the substrate potential cannot easily be changed in an atomic system. Our system can be understood as a special case of an atomic adsorbate system exposed to a 1D substrate potential, but

possesses the additional advantage of an adjustable “substrate potential.”

In summary, we have studied the phase transition of a 2D colloidal system subjected to a 1D spatially modulated light potential. We have demonstrated that, as the light potential is gradually increased, a 2D liquid first crystallizes in predominantly hexagonal order and then melts again to a modulated liquid. This reentrant melting is in agreement with theoretical predictions.

We acknowledge valuable discussions with J. Chakrabarti and the help of S. Naser with the image processing program. One of the authors (Q. H. W.) would like to thank the Alexander von Humboldt Foundation for financial support. The work was supported by the Deutsche Forschungsgemeinschaft (SFB 513).

- 
- [1] For a review, see K. J. Strandburg, *Rev. Mod. Phys.* **60**, 161 (1988); H. Löwen, *Phys. Rep.* **237**, 249 (1994).
  - [2] N. A. Clark, B. J. Ackerson, and A. J. Hurd, *Phys. Rev. Lett.* **50**, 1459 (1983).
  - [3] T. V. Ramakrishnan and M. Yussouff, *Phys. Rev. B* **19**, 2775 (1979); T. V. Tamakrishnan, *Phys. Rev. Lett.* **48**, 541 (1982); A. D. J. Haymet and D. Oxtoby, *J. Chem. Phys.* **74**, 2559 (1981); for a review, see Y. Singh, *Phys. Rep.* **207**, 351 (1991).
  - [4] A. Chowdhury, B. J. Ackerson, N. A. Clark, *Phys. Rev. Lett.* **55**, 833 (1985).
  - [5] J. Chakrabarti, H. R. Krishnamurthy, and A. K. Sood, *Phys. Rev. Lett.* **73**, 2923 (1994).
  - [6] J. Chakrabarti, H. R. Krishnamurthy, A. K. Sood, and S. Sengupta, *Phys. Rev. Lett.* **75**, 2232 (1995).
  - [7] K. Loudiyi and B. J. Ackerson, *Physica (Netherlands)* **184A**, 1–25 (1992); *ibid.* **184A**, 26–41 (1992).
  - [8] M. T. Palberg, W. Härtl, U. Wittig, H. Versmold, and H. Würth, *J. Phys. Chem.* **96**, 8081 (1992).
  - [9] Q.-H. Wei, C. Bechinger, D. Rudhardt, and P. Leiderer, *Prog. Colloids Interface Sci.* **110**, 46 (1998).
  - [10] D. C. Prieve, S. G. Biko, and N. A. Frej, *Faraday Discuss. Chem. Soc.* **90**, 209 (1990).
  - [11] D. Rudhardt, C. Bechinger, and P. Leiderer, *Prog. Colloids Interface Sci.* **110**, 37 (1998).
  - [12] J. Chakrabarti and S. Sinha, *J. Phys. II (France)* **7**, 729 (1997).
  - [13] N. D. Mermin, *Phys. Rev.* **176**, 250 (1968).
  - [14] D. R. Nelson and B. I. Halperin, *Phys. Rev. B* **19**, 2457 (1979).
  - [15] G. Dash, *Films on Solid Surfaces* (Academic, New York, 1975).
  - [16] See Fig. 12 in Ref. [14].